

Polymers **2011**, *3*, 114-130; doi:10.3390/polym3010114

OPEN ACCESS

polymers

ISSN 2073-4360

www.mdpi.com/journal/polymers

Article

Gelatin Functionalization of Biomaterial Surfaces: Strategies for Immobilization and Visualization

Sandra Van Vlierberghe, Els Vanderleyden, Veerle Boterberg and Peter Dubruel *

Polymer Chemistry & Biomaterials Research Group, Ghent University, Krijgslaan 281 S4-bis, 9000 Ghent, Belgium; E-Mails: sandra.vanvlierberghe@ugent.be (S.V.); els.vanderleyden@ugent.be (E.V.); veerle.boterberg@ugent.be (V.B.)

* Author to whom correspondence should be addressed; E-Mail: Peter.Dubruel@UGent.be; Tel.: 003292644466; Fax: 003292644972.

Received: 11 November 2010; in revised form: 10 December 2010 / Accepted: 31 December 2010 / Published: 5 January 2011

Abstract: In the present work, the immobilization of gelatin as biopolymer on two types of implantable biomaterials, polyimide and titanium, was compared. Both materials are known for their biocompatibility while lacking cell-interactive behavior. For both materials, a pre-functionalization step was required to enable gelatin immobilization. For the polyimide foils, a reactive succinimidyl ester was introduced first on the surface, followed by covalent grafting of gelatin. For the titanium material, methacrylate groups were first introduced on the Ti surface through a silanization reaction. The applied functionalities enabled the subsequent immobilization of methacrylamide modified gelatin. Both surface modified materials were characterized in depth using atomic force microscopy, static contact angle measurements, confocal fluorescence microscopy, attenuated total reflection infrared spectroscopy and X-ray photo-electron spectroscopy. The results indicated that the strategies elaborated for both material classes are suitable to apply stable gelatin coatings. Interestingly, depending on the material class studied, not all surface analysis techniques are applicable.

Keywords: gelatin immobilization; polyimide; titanium; surface characterization

1. Introduction

Surface modification of biomaterials to improve the final biocompatibility and/or the cell-interactive behavior of implants has gained increasing interest over the last decades [1-5]. Langer *et al.* modified the surface of poly(glycerol-*co*-sebacic acid) membranes with peptides containing an RGD ligand sequence to improve the attachment of photoreceptor layers in the retina [6]. Neff *et al.* modified polystyrene surfaces with GRGDSY (*i.e.*, a cell adhesion motif) using a PEO/PPO/PEO triblock copolymer spacer [7,8]. The results indicated that cell adhesion and subsequent spreading was improved significantly. The research group of Hubbell has also reported on the RGD functionalization of several polymers including poly(ethylene glycol), polyethylene terephthalate and polytetrafluoroethylene in order to improve cell attachment [9,10]. Stupp *et al.* have biofunctionalized various surfaces including nickel-titanium alloys and poly(L-lactic acid) scaffolds with self-assembled peptide amphiphile (PA) nanofibers possessing bioactive functions including RGD sequences [11-14]. The research group of Textor has improved the adhesion of osteoblasts on titanium surfaces via an RGD-containing non-fouling poly((L)-lysine)-*graft*-poly(ethylene glycol) molecular assembly system.[15] In addition, adequate surface modification of polymer matrices is also essential to enable appropriate cell differentiation as indicated by Vacanti *et al.* [16] Zhu *et al.* obtained an endothelial cell proliferation increase by applying amines and gelatin on polyester-type polyurethane scaffolds [17]. In the present work, we report on the biofunctionalization of different implant materials including polyimide (PI) and titanium (Ti). PIs are polymers possessing various interesting properties including high strength, bio-inertness and -resistance, electrical insulation and full compatibility with device fabrication processes [18]. The biocompatibility of PI was already reported on earlier using *in vitro* assays which indicated that PI implants only showed a limited coagulation and a minor cytotoxicity and hemolysis [19]. Up to now, PI-based microdevices have already been applied as stable, neural implants preserving their properties for several months [20-22]. However, since the success or failure of an implant mainly depends on the interactions that occur at the tissue-implant interface, gelatin was selected as the polymer coating in order to improve the cell-interactive properties of the different selected implant materials. Previously, our research group reported on the potential of gelatin-based scaffolds for tissue engineering due to their cell-interactive properties [23-26]. In those recent papers, gelatin was applied as such. In the present work, we however aim at applying gelatin as implant coating material for both polyimide and titanium. Both materials are biocompatible but lack the required cell-interactive properties.

A previous study from our research group already reported on the surface activation of polyimide (PI) sheets using two surface modification strategies [27]. In the first methodology, crosslinkable vinyl groups were introduced on the polyimide surface using aminopropylmethacrylamide. In the second approach, a reactive succinimidyl ester was introduced on the surface of PI. Using the former approach, the aim was to apply a vinyl functionalized biopolymer coating. In the latter approach, any amine containing biopolymer can be immobilized. The surface-modified PI sheets were developed to be applied as implants for ocular diseases including age-related macular degeneration (AMD), which is an illness causing blindness among elderly people in the western world. The present work reports on both the surface modification and in depth characterization of these PI foils. In order to improve the

cell interactive property of this material, reactive succinimidyl esters will be introduced on the PI surface enabling the subsequent coupling of gelatin.

In an alternative two step procedure, we also surface modified titanium (Ti) using gelatin. Ti has gained large interest as a load-bearing scaffold material for bone tissue engineering [28-30]. In order to realize bone healing, osseointegration of the metal implant in the surrounding tissue has to be achieved. This process can be stimulated by surface immobilization of peptides, proteins or growth factors. Up to now, different methods have been proposed for enabling gelatin immobilization on Ti-surfaces [31,32]. Weng *et al.* have reported on the coupling of azide-functionalized gelatin to Ti-O surfaces obtained using unbalanced magnetron sputtering [31]. They showed that the surface modification enabled the attachment of human endothelial cells. Kuangl *et al.* applied 2-hydroxyethyl acrylate on a titanium surface to couple gelatin [32]. The scaffolds developed exhibited interesting mineralization properties. In addition, they observed that bovine serum albumin adhered to a great extent to the surface-functionalized scaffolds. In the present work, we will introduce double bonds on Ti-surfaces using silanization [33]. These functional groups will subsequently be applied to enable gelatin immobilization on the modified Ti-surfaces.

The present paper focuses on an in depth comparison of the surface functionalization of two implantable materials including polymers (*i.e.*, polyimide) and metals (*i.e.*, titanium).

2. Experimental

2.1. Development of Gelatin-Coated Polyimide Foils

The polyimide (PI) foils (Pyralin PI 2611, HD Microsystems, Bad Homburg, Germany) were developed as described earlier [27]. In brief, a polyimide (PI) foil (1 cm × 1 cm, 10 μm thick) was incubated at ambient temperature in 1 mL ethyl acetate (Acros) for 4 hours in the presence of the succinimidyl ester of 4-azido-2,3,5,6-tetrafluorobenzoic acid (AFB) (5 mg/mL, Invitrogen) protected from light. Next, the PI foil was irradiated for 15 minutes with UV-C lamps (250 nm, TUV 15W/G15 T8, Philips), followed by two washing steps with ethyl acetate and phosphate buffer (pH 8) yielding succinimidyl ester-modified PI foils (PI-AFB).

Next, the modified foils were incubated in an aqueous gelatin (type B, MW 155 kDa, polydispersity 2.5) solution (5 w/v%, pH 8) at 40 °C for 3 hours. In a final step, the foils were incubated in double distilled water at 40 °C for three hours to remove the physically adsorbed (*i.e.*, non covalently bound) gelatin.

2.2. Development of Gelatin-Coated Titanium

Methacrylamide-modified gelatin (type B, MW 155 kDa, polydispersity 2.5) (Gel-mod) was prepared as described previously [34]. Briefly, the amine groups in gelatin were chemically modified with methacrylamide moieties, resulting in a degree of substitution (DS) of 78% relative to the original content of primary amines [34].

The pre-treatment and silanisation of the Ti samples was performed as described previously [28]. In brief, the Ti samples were degreased and the native oxide layer was etched before treatment with an oxidizing agent. Next, the oxidized Ti samples were silanized using a 3-(trimethoxysilyl)propyl

methacrylate (TMSPMA) solution (10 v/v% in pentane). The samples were then dipcoated in a Gel-mod solution (10 w/v%, in milliQ-water), containing the photoinitiator Irgacure® 2959 (2 mol% relative to the amount of crosslinkable groups) at 40 °C. In a final step, the samples were irradiated with UV-C lamps (250 nm, TUV 15W/G15 T8, Philips) for 30 min. In a final step, the gelatin-coated Ti samples were incubated in double distilled water at 40 °C for three hours to remove the physically adsorbed (*i.e.*, non covalently bound) gelatin.

2.3. Characterization of Surface-Modified Biomaterials

2.3.1. Static Contact Angle Measurements

For each static contact angle measurement (SCA), 1 µL of double distilled water was placed on the (un)modified PI surface at room temperature. For the Ti samples a drop volume of 2 µL was used. The spreading of the droplet was imaged using a video camera using 1 frame/second. The contact angle was determined based upon the Laplace Young fitting using the imaging software provided by the supplier (SCA 20, version 2.1.5 build 16).

2.3.2. Atomic Force Microscopy

Atomic force microscopy studies were performed with a Nanoscope IIIa Multimode equipped with 4.43r8 software (Digital Instruments, Santa Barbara, California, U.S.) applying ‘tapping mode’ in air. Changes in surface morphology are quantified by root-mean-square (RMS) roughness values (R_q). The RMS roughness is defined as follows:

$$R_q = \sqrt{\frac{(Z_i - Z_{ave})^2}{N}} \quad (1)$$

where Z_{ave} is the average Z height value within a given area, Z_i is the current Z value and N is the number of points within the given area.

2.3.3. X-ray Photo-Electron Spectroscopy

The chemical composition of the biomaterial surfaces was determined using FISON S-PROBE, a dedicated X-ray photo-electron microscopy (XPS) instrument designed to give an ultimate performance, while providing a high sample throughput. The fine focus Al-Ka source with a quartz monochromator, developed by Fisons Instruments Surface Science ensures lower background and higher sensitivity than conventional twin anode sources. All measurements were performed in a vacuum of at least 10^{-9} Pa. Wide and narrow-scan spectra were acquired at pass energy of 158 and 56 eV respectively. The binding energy was calibrated by the C 1 s peak at 284.6 eV. The spot size used was 250 µm on 1 mm. Data analysis was performed using S-PROBE software. The measured spectrum was displayed as a plot of the number of electrons (electron counts) *versus* electron binding energy in a fixed, small energy interval. Peak area and peak height sensitivity factors were used for the quantifications. All data are expressed as atomic %.

2.3.4. Attenuated Total Reflectance Infrared (ATR-IR) Spectroscopy

The ATR-IR measurements were performed using a Spectrum 100 FT-IR Spectrometer (Perkin Elmer) combined with a Spotlight 400 FT-IR Imaging System (Perkin Elmer). The crystal in the ATR module is Ge. Mapping is possible with a pixel size of 6.25 or 1.56 μm .

2.3.5. Confocal Fluorescence Microscopy (CFM)

To enable CFM analysis, gelatin was labeled with either Texas Red (Texas Red®-X, succinimidyl ester, mixed isomers, Invitrogen) or Oregon Green (Oregon Green® 488-X, succinimidyl ester, 6-isomer, Invitrogen). Images were collected in wet conditions. The confocal images of the gelatin coatings on the biomaterials surfaces were collected on a Leica SP5 laser scanning confocal microscope with a 40 \times 1.25 oil immersion objective. Digital Z series were reconstructed using Velocity image analysis software.

2.3.6. Statistical Analysis

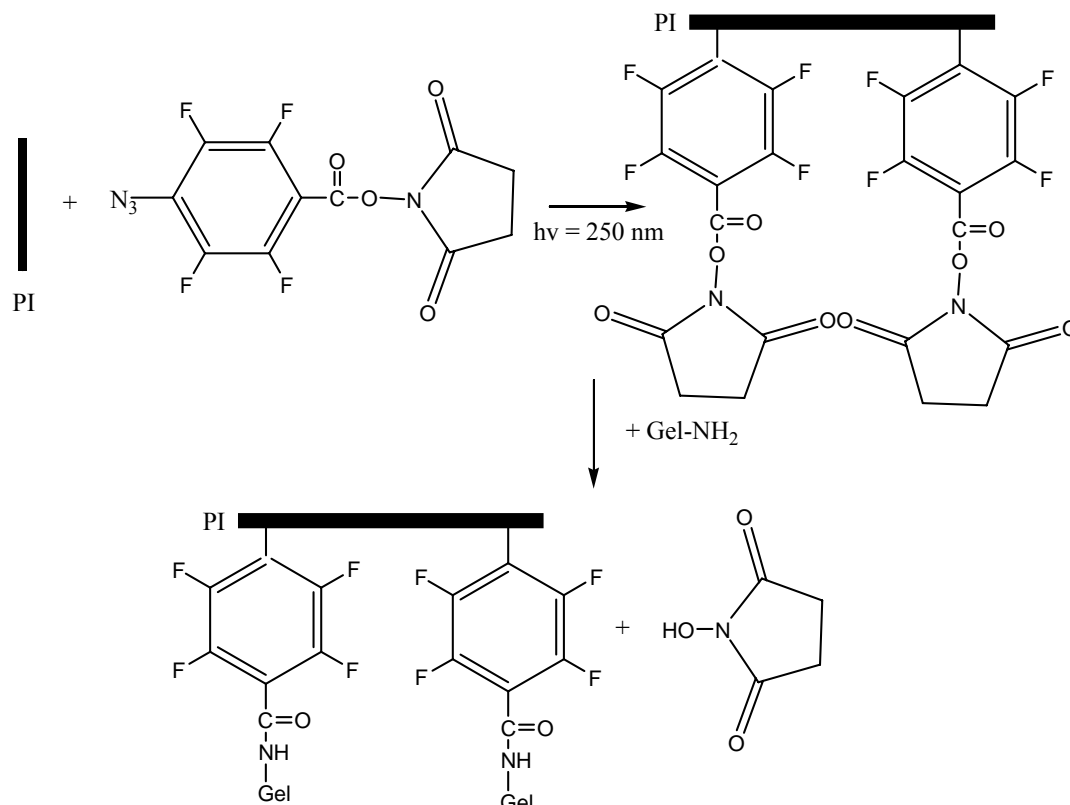
Possible significant differences among groups were studied with the Student's *t* test by a two-population comparison. Statistical significance was considered at a probability of $P < 0.05$.

3. Results & Discussion

3.1. Development and Characterization of Gelatin-Coated Polyimide Foils

In a first part of the present work, the development and characterization of gelatin-coated polyimide (PI) foils was studied. In order to surface-activate PI, reactive ester groups were introduced on the PI surface using the succinimidyl ester of 4-azido-2,3,5,6-tetrafluorobenzoic acid (AFB) as heterobifunctional reagent (see Figure 1). Via its azide group, AFB can be coupled to the PI surface under UV illumination. This approach enables the subsequent direct coupling of any amine-containing biomolecule such as gelatin using the reactive ester moieties introduced in the first step. The heterobifunctional derivative selected was already applied successfully to immobilize reactive ester groups on polymer surfaces [27,35,36]. In addition, azide-containing compounds were previously immobilized on Kapton films (*i.e.*, poly-oxydiphenylene-pyromellitimide) by Harmer [37]. The UV light is required to enable conversion of the tetrafluorophenylazido group to phenylnitrene. This highly reactive compound forms covalent linkages with the PI as well as neighboring AFB molecules leading to the formation of a polymeric multilayer. In addition, the nitrene intermediates can also lead to the formation of amines, nitro or nitroso compounds and even ring expansion is possible [38]. However, these side products are removed during the washing step [38]. Therefore, the reaction between nitrene and alkyl C-H bonds from neighboring AFB molecules is anticipated to occur more frequently [39]. The mechanism was already elucidated before by our research group [27].

Figure 1. Reaction scheme for the immobilization of gelatin on the PI surface using the succinimidyl ester of AFB.



The modified foils were characterized using a variety of techniques. Static contact angle (SCA) measurements (Figure 2) indicate that the SCA of PI-AFB did not significantly differ from that of blank PI ($P > 0.05$). However, after applying a gelatin coating, the SCA decreased from 59° to 49° ($P < 0.05$), as anticipated based on the hydrophilicity increase of the surface after immobilizing gelatin. In addition to SCA measurements, atomic force microscopy (AFM) analysis was performed to study possible morphological alterations induced on the PI surface after reaction with the succinimidyl ester of AFB and/or the subsequent gelatin immobilization. As indicated in Figure 3, the chemical modification significantly alters the PI surface morphology. The non-modified PI foil possesses a smooth surface with no distinguishable features (see Figure 3(a)), while the surface of PI-AFB shows a large number of nano-scale depressions (see Figure 3(b)). After applying a gelatin coating, the size of the nano-scale depressions decreases to a certain extent (see Figure 3(c)), which is also illustrated by the root-mean-square roughness values (R_{rms}). Blank PI has an R_{rms} value of 0.5 nm, while PI-AFB and gelatin-coated PI possess an R_{rms} value of 3.3 nm and 1.9 nm respectively (see Table 1). We hypothesize that gelatin fills up the nano-scale depressions on the surface-activated PI to a certain extent. Therefore, the final surface roughness is determined by both the gelatin coating as well as by the surface-activation on PI using the succinimidyl ester of AFB. Furthermore, the surface plot of the gelatin-coated PI (see Figure 3(c)) clearly indicates the absence of globular domains, which is atypical for proteins deposited on a surface. We therefore now aim at elucidating the effect of this protein conformation on the subsequent cell adhesion, spreading and proliferation using *in vitro* biocompatibility assays. The results of this study will be the topic of a forthcoming paper. This is highly relevant since, as an example, Guerra *et al.* already reported on the influence of fibronectin

conformations on the subsequent cell attachment [40]. We thus anticipate that the gelatin conformation will also significantly affect the subsequent cell adhesion.

Figure 2. Static contact angle measurements of blank (PI), ester-modified (PI-AFB) and gelatin-coated PI (PI-AFB + Gel). The values obtained are an average of three separate measurements.

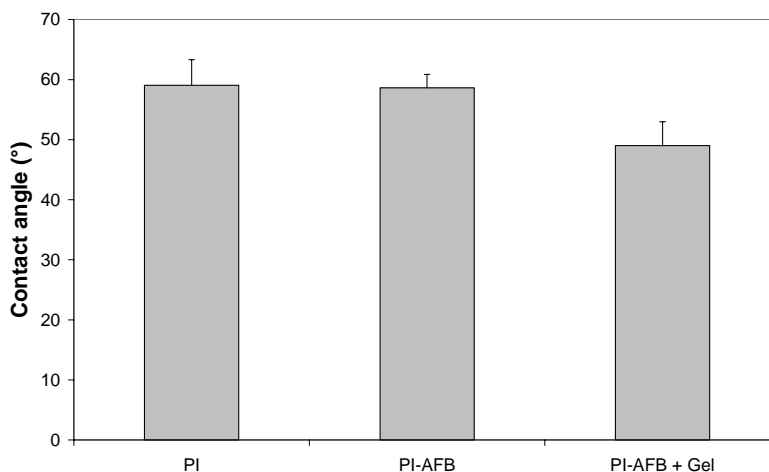


Figure 3. AFM images of (a) unmodified PI, (b) PI modified with the succinimidyl ester of AFB (PI-AFB) and (c) PI coated with gelatin.

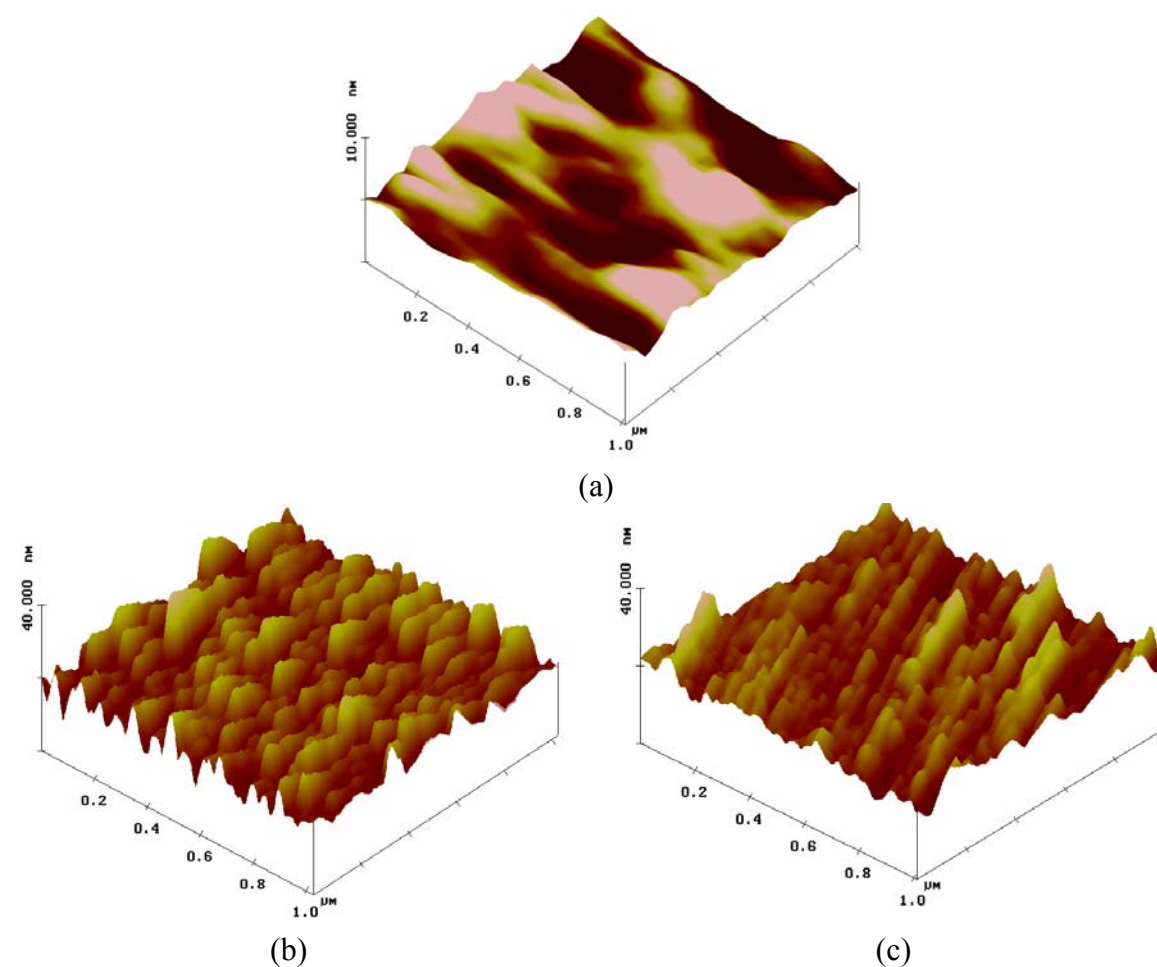


Table 1. Surface roughness values (Rms) of PI, PI-AFB and gelatin-coated PI obtained using AFM analysis.

	Rms (Rq)
PI	0.5 nm
PI-AFB	3.3 nm
PI-AFB + Gel	1.9 nm

In a subsequent part of the material surface analysis, X-ray photoelectron spectroscopy (XPS) was applied to analyze the obtained differences in chemical composition between non- and surface-modified PI. Table 2 indicates the presence of 1% F after reaction with AFB, due to the presence of fluorine in the grafted AFB moieties. In addition, a nitrogen increase from 6% to 11% was observed when comparing PI-AFB and gelatin-coated PI respectively, which proves the successful protein deposition on the PI surface.

Table 2. Atomic surface composition of PI, PI-AFB and gelatin-coated PI acquired by means of XPS.

	PI	PI-AFB	PI-AFB + Gel
C	79%	72%	69%
N	5%	6%	11%
O	16%	21%	19%
F	-	1%	1%
O/C	0.20	0.29	0.26
N/C	0.06	0.08	0.16

The successful gelatin grafting was also further confirmed using ATR-IR mapping (see Figure 4). The ATR-IR spectrum of gelatin is mainly characterized by the presence of two important characteristic regions (*i.e.*, the amide I and the amide II band) [41]. The amide I band, which is due primarily to C=O stretching of the peptide groups, is extremely sensitive to changes in the gelatin chain conformation. The wavenumber of the characteristic band of these carbonyl groups is determined by the local chemical environment and the degree of dipole-dipole interaction between neighboring carbonyl groups [42]. The band at $1,664\text{ cm}^{-1}$ is related to the presence of both triple helices and β -turns [42]. The amide II region consists of a band at $1,556\text{ cm}^{-1}$ (*i.e.*, NH bend coupled with CN stretch) [43]. The two characteristic protein peaks at $1,556$ and $1,664\text{ cm}^{-1}$ are also present in the IR-spectrum of gelatin-modified PI (data not shown). In order to study whether the PI surface was completely biofunctionalized with gelatin, ATR-IR maps ($100\text{ }\mu\text{m} \times 100\text{ }\mu\text{m}$) were recorded at $1,556\text{ cm}^{-1}$ (Figure 4(a)) and $1,664\text{ cm}^{-1}$ (Figure 4(b)). The IR maps clearly indicate that gelatin is indeed present throughout the entire PI surface. As a final surface analysis technique, confocal fluorescence microscopy (CFM) measurements were performed to visualize surface immobilized texas red-labeled gelatin. The results (see Figure 5) indicate that without PI activation, texas red-labeled gelatin is not grafted on the PI surface (Figure 5(a)). When applying the labeled gelatin on PI-AFB, the CFM analysis clearly showed the complete coverage of the PI surface with gelatin (Figure 5(b)).

Figure 4. Attenuated Total Reflection Infrared (ATR-IR) maps showing the IR absorbance of the gelatin-coated PI at (a) $1,556\text{ cm}^{-1}$ and (b) $1,664\text{ cm}^{-1}$.

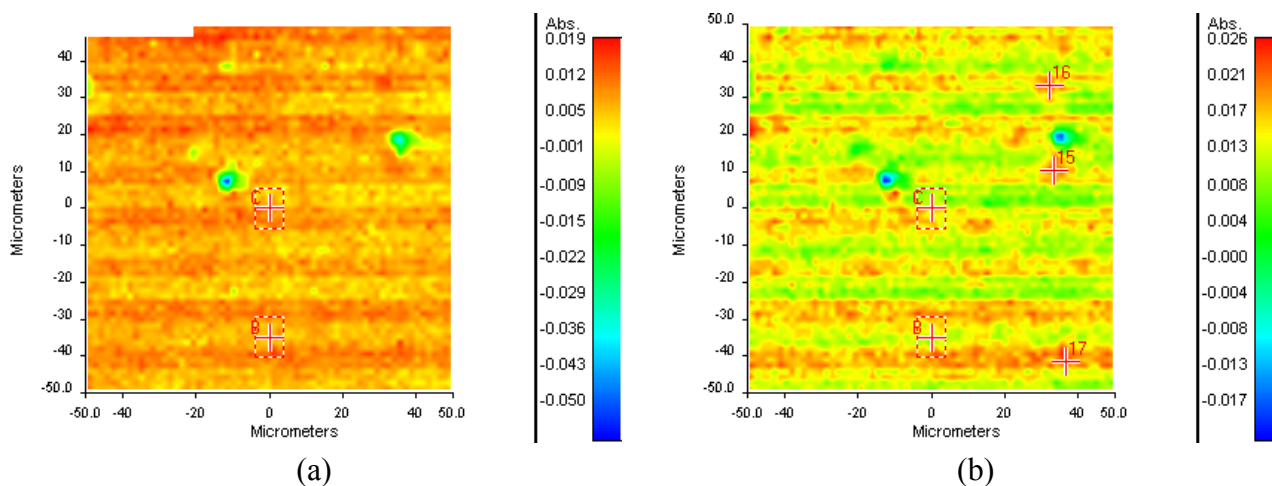
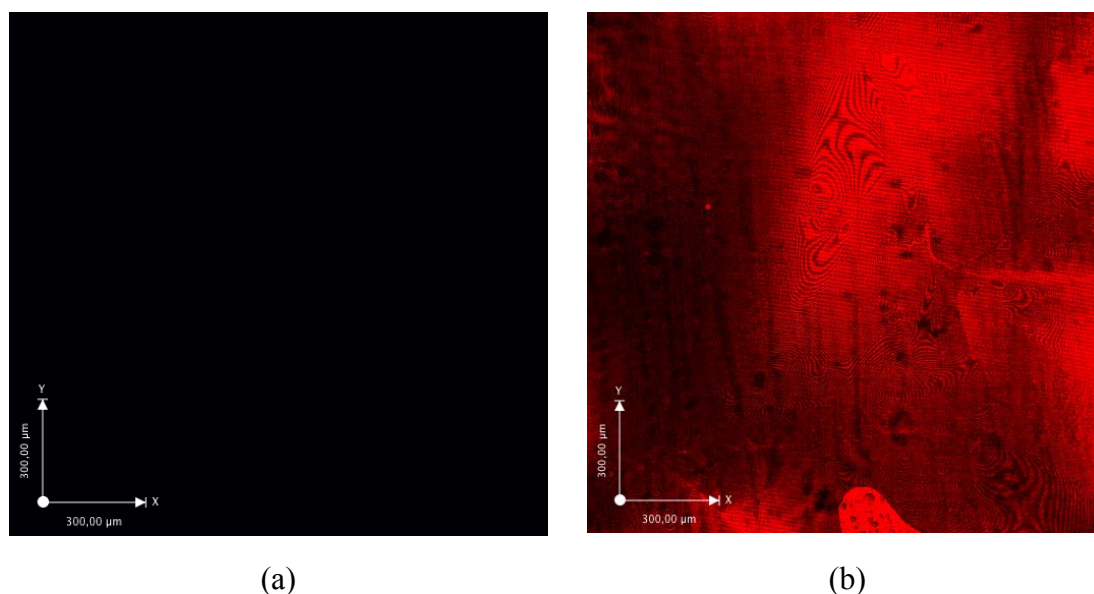


Figure 5. Confocal fluorescence microscopy images of non-modified PI (a) and texas red-labelled gelatin-coated PI (b).



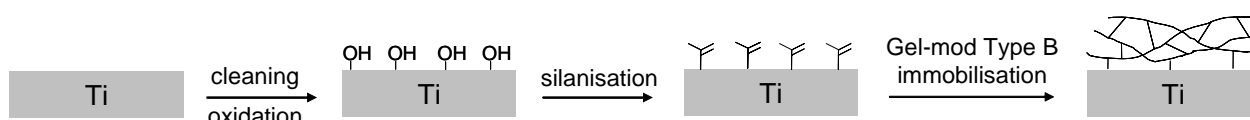
The different characterization techniques applied thus enabled us to safely conclude that the PI modification with succinimidyl ester functionalities and the subsequent gelatin immobilization was successful.

3.2. Development and Characterization of Gelatin-Coated Titanium

In a second part of the present work, we aimed at applying a gelatin coating on a Ti surface in order to improve the final *in vitro* and *in vivo* cell-interactive properties of Ti implants. The procedure comprised two steps, now also involving a polymer modification step. In a first step, gelatin was modified using methacrylic anhydride in order to introduce polymerizable methacrylamide moieties, as

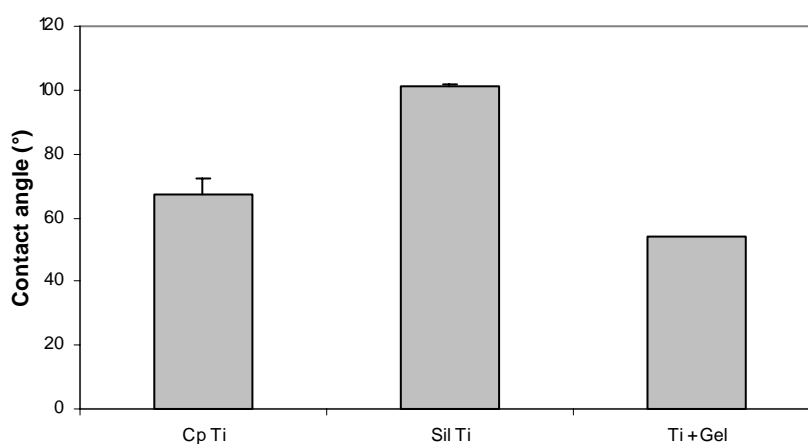
described earlier [34]. Next, the Ti samples were cleaned, oxidized and silanized using TMSPPMA in order to surface-functionalize the samples with polymerizable methacrylate groups. The gelatin immobilization was performed by dipcoating the silanized Ti samples in a Gel-mod solution containing Irgacure 2959, under UV-irradiation. The grafting strategy elaborated in the present work is illustrated in Figure 6. As with the modified PI foils, the modified surfaces were characterized in depth using a variety of surface (imaging) techniques.

Figure 6. Overview of gelatin immobilization on commercially pure Ti (cp Ti).



SCA measurements (see Figure 7) indicated a contact angle increase from 67° for a commercially pure (cp) Ti surface to 101° for a TMSPPMA silanized Ti surface (Sil Ti) ($P < 0.05$). The latter was anticipated based on the hydrophobic nature of the propyl and the methacrylate functionality of TMSPPMA. After gelatin immobilization, a contact angle of 54° was obtained confirming the presence of the more hydrophilic protein layer on the Ti surface.

Figure 7. Static contact angle measurements of cp Ti, TMSPPMA silanized Ti (Sil Ti) and gelatin-coated Ti (Ti + Gel). The values obtained are an average of three separate measurements.



In order to study possible morphological changes of the Ti surface upon surface modification, AFM measurements were performed (see Figure 8). The cleaning, the oxidation and the subsequent silanization procedure influenced the Ti surface morphology to a great extent. An overall increase in surface roughness was observed from 66 nm for cp Ti to 190 nm for silanized Ti (see Table 3). This is mainly due to the formation of TMSPPMA aggregates during the silanization reaction (Figure 8(b)). After gelatin immobilization, the surface roughness decreased to 95 nm (Table 3, Figure 8(c)). We anticipate that the final surface roughness is determined by the gelatin layer. As a result, cell attachment will mainly depend on both the surface roughness as well as on the gelatin conformation. Similar to the PI samples, *in vitro* biocompatibility studies will be performed to further study the effect

of these phenomena. We thus anticipate that the tissue engineering field would benefit significantly from fine-tuning the coating thickness in such a way that, in this case, the gelatin degradation profile matches the formation of new bone within the porous Ti scaffold.

Figure 8. AFM images of (a) cp Ti, (b) TMSPMA silanized Ti and (c) gelatin-coated Ti.

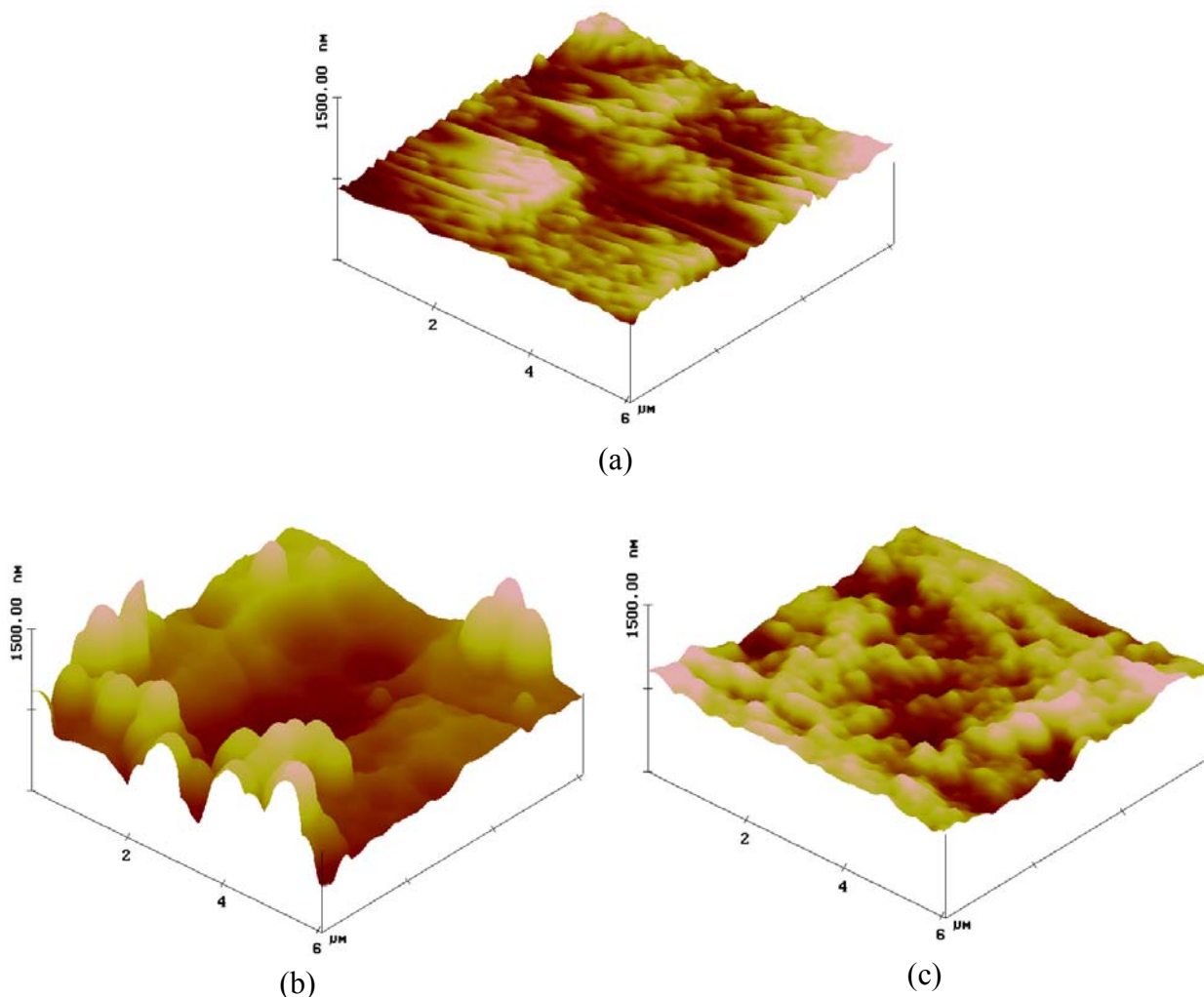


Table 3. Surface roughness values (Rms) of commercially pure Ti (cp Ti), TMSPMA silanized Ti (Sil Ti) and gelatin-coated Ti obtained using AFM analysis.

	Rms (Rq)
Cp Ti	66 nm
Sil Ti	190 nm
Ti + Gel	95 nm

Next, the influence of the modification on the chemical composition of the Ti surface was determined using XPS measurements. Table 4 summarizes the atomic surface compositions of a cp Ti surface, a silanized Ti surface and a gelatin-coated Ti surface. After silanization, 9% Si was detected on the surface while the Ti signal disappeared. The latter indicated a complete coverage of the Ti surface by TMSPMA. The subsequent gelatin immobilization was confirmed by the presence of a N

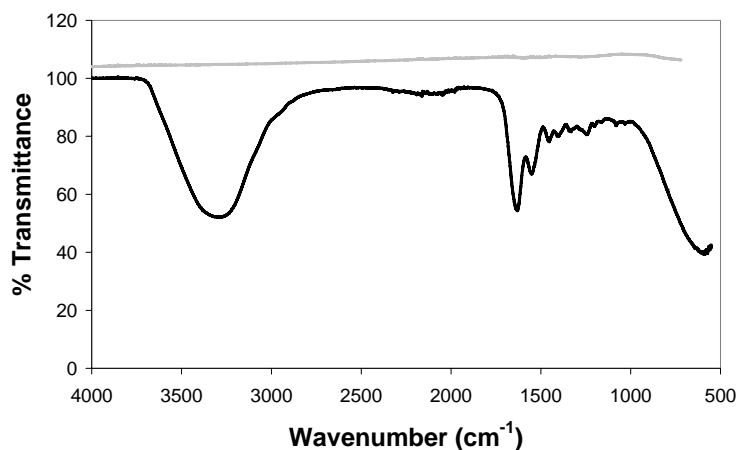
signal. The atomic composition of the modified Ti surface resembled the composition of a pure Gel-mod hydrogel.

Table 4. Atomic surface composition of commercially pure Ti (cp Ti), TMSPMA silanized Ti and gelatin-coated Ti acquired by means of XPS.

	Cp Ti	Sil Ti	Ti + Gel
Ti	3%	-	-
C	68%	59%	66%
N	3%	-	11%
O	25%	31%	21%
Si	-	9%	2%
O/C	0.37	0.53	0.32
N/C	0.04	-	0.17

Very interestingly, and in contrast to the PI foils included in this work (§ 3.1), ATR-IR could not be applied on the silanized Ti samples. Our current working hypothesis is that the siloxane layer is thinner than the penetration depth of the laser (see Figure 9). After applying the gelatin coating, the spectrum obtained resembles the one of Gel-mod (Figure 9). In this case, the thickness of the gelatin coating exceeds the penetration depth of the IR laser and reflection is avoided.

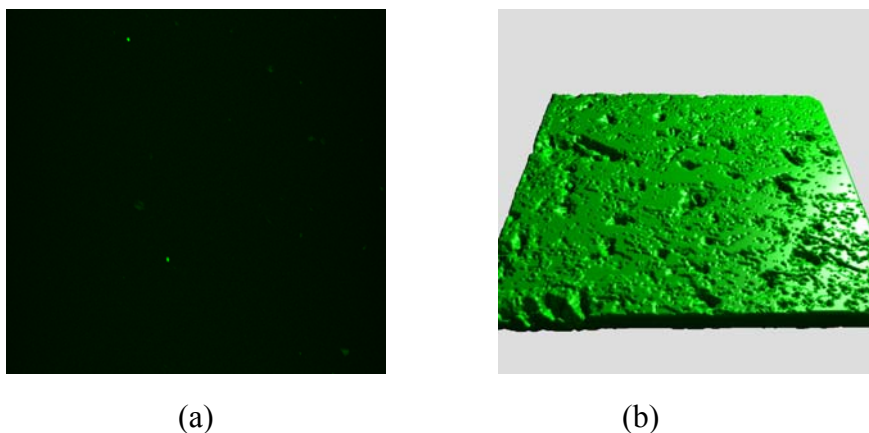
Figure 9. ATR-IR spectra of cp Ti (grey) and gelatin-coated Ti (black).



In addition to AFM, the gelatin coating was also visualized by means of CFM after staining the gelatin coating using Oregon Green (see Figure 10). Figure 10(b) illustrates the presence of a homogeneous gelatin coating on the Ti surface, in contrast to the control sample (*i.e.*, an Oregon Green-stained cp Ti sample (Figure 10(a))).

As with the modified PI samples (§ 3.1), it can again be concluded that the different characterization techniques clearly indicated a successful modification of Ti with methacrylate moieties and its subsequent functionalization using gelatin with polymerizable side groups.

Figure 10. Confocal fluorescence microscopy images (magnification 63X) of cp Ti (**a**) and Oregon Green-labeled gelatin-coated Ti (isosurface mode, **b**).



4. Conclusions

In the present work, two biocompatible implant materials were surface-functionalized with gelatin with the aim to increase their cell-interactive properties. The materials included polyimide (PI) Pyralin PI 2611 as polymer, and titanium as metal. Although both materials possess completely different properties, including physico-chemical and mechanical characteristics, a bioactive gelatin coating was successfully applied on both surfaces by varying the immobilization procedure. Polyimide can be processed into thin, porous membranes to be applied for retinal tissue engineering applications while porous titanium scaffolds are suitable for load-bearing applications including bone tissue engineering. However, the presence of a cell-interactive coating on the surface of both materials is essential when aiming at tissue regeneration. In a first part, gelatin was immobilized on the PI surface after modification of the surface using the succinimidyl ester of 4-azido-2,3,5,6-tetrafluorobenzoic acid. Secondly, the titanium surface was also biofunctionalized with gelatin after an initial silanization step using TMSPPMA. Various characterization techniques including atomic force microscopy, static contact angle measurements, X-ray photo-electron spectroscopy, attenuated total reflection infrared spectroscopy (ATR-IR) and confocal fluorescence microscopy indicated that the methodologies developed for the gelatin immobilization were successful. Interestingly, ATR-IR cannot be applied on titanium samples.

The present work is highly relevant for tissue engineering applications and, more specifically, for implant materials of which a good integration in the surrounding tissue is essential to realize a successful *in vivo* biological performance. Future work will include a detailed biological evaluation of the surface modified PI and Ti implant materials. The *in vitro* and *in vivo* biocompatibility results will be the topic of two forthcoming papers.

Acknowledgement

The authors would like to acknowledge the PolExGene consortium. PolExGene is a STREP project (contract number 019114) funded under the EU 6th framework programme. Sandra Van Vlierberghe is post-doctoral fellow of the Research Foundation-Flanders (FWO, Belgium). Further acknowledgement

goes to the Agency for Innovation by Science and Technology in Flanders (IWT). The authors would like to thank Christopher J. Guérin, leader of the microscopy core facility of the Flemish Institute of Biotechnology, Department of Molecular Biomedical Research, for the CFM images, and Raymond Kemps from the Flemish Institute for Technological Research (VITO) for the SEM images.

References

1. Desmet, T.; Morent, R.; De Geyter, N.; Leys, C.; Schacht, E.; Dubruel, P. Nonthermal Plasma Technology as a Versatile Strategy for Polymeric Biomaterials Surface Modification: A Review. *Biomacromolecules* **2009**, *10*, 2351-2378.
2. Van Vlierberghe, S.; Vanderleyden, E.; Dubruel, P.; De Vos, F.; Schacht, E. Affinity Study of Novel Gelatin Cell Carriers for Fibronectin. *Macromol. Biosci.* **2009**, *9*, 1105-1115.
3. Vepari, C.; Matheson, D.; Drummy, L.; Naik, R.; Kaplan, D.L. Surface Modification of Silk Fibroin with Poly(ethylene glycol) for Antiadhesion and Antithrombotic Applications. *J. Biomed. Mater. Res. A* **2010**, *93A*, 595-606.
4. Zhu, Y.B.; Chian, K.S.; Chan-Park, M.B.; Mhaisalkar, P.S.; Ratner, B.D. Protein Bonding on Biodegradable Poly(L-lactide-co-caprolactone) Membrane for Esophageal Tissue Engineering. *Biomaterials* **2006**, *27*, 68-78.
5. LaNasa, S.M.; Bryant, S.J. Influence of ECM Proteins and Their Analogs on Cells Cultured on 2-D Hydrogels for Cardiac Muscle Tissue Engineering. *Acta Biomater.* **2009**, *5*, 2929-2938.
6. Pritchard, C.D.; Arner, K.M.; Neal, R.A.; Neeley, W.L.; Bojo, P.; Bachelder, E.; Holz, J.; Watson, N.; Botchwey, E.A.; Langer, R.S.; Ghosh, F.K. The Use of Surface Modified Poly(glycerol-co-sebacic acid) in Retinal Transplantation. *Biomaterials* **2010**, *31*, 2153-2162.
7. Neff, J.A.; Caldwell, K.D.; Tresco, P.A. A Novel Method for Surface Modification to Promote Cell Attachment to Hydrophobic Substrates. *J. Biomed. Mater. Res.* **1998**, *40*, 511-519.
8. Neff, J.A.; Tresco, P.A.; Caldwell, K.D. Surface Modification for Controlled Studies of Cell-Ligand Interactions. *Biomaterials* **1999**, *20*, 2377-2393.
9. VandeVondele, S.; Voros, J.; Hubbell, J.A. RGD-Grafted Poly-l-lysine-graft-(polyethylene glycol) Copolymers Block Non-Specific Protein Adsorption While Promoting Cell Adhesion. *Biotechnol. Bioeng.* **2003**, *82*, 784-790.
10. Massia, S.P.; Hubbell, J.A. Human Endothelial-Cell Interactions with Surface-Coupled Adhesion Peptides on a Nonadhesive Glass Substrate and 2 Polymeric Biomaterials. *J. Biomed. Mater. Res.* **1991**, *25*, 223-242.
11. Bansiddhi, A.; Sargeant, T.D.; Stupp, S.I.; Dunand, D.C. Porous NiTi for Bone Implants: A Review. *Acta Biomater.* **2008**, *4*, 773-782.
12. Hartgerink, J.D.; Beniash, E.; Stupp, S.I. Peptide-Amphiphile Nanofibers: A Versatile Scaffold for the Preparation of Self-Assembling Materials. *Proc. Natl. Acad. Sci. USA* **2002**, *99*, 5133-5138.
13. Sargeant, T.D.; Rao, M.S.; Koh, C.Y.; Stupp, S.I. Covalent Functionalization of NiTi Surfaces with Bioactive Peptide Amphiphile Nanofibers. *Biomaterials* **2008**, *29*, 1085-1098.
14. Stendahl, J.C.; Li, L.M.; Claussen, R.C.; Stupp, S.I. Modification of Fibrous Poly(L-lactic acid) Scaffolds with Self-Assembling Triblock Molecules. *Biomaterials* **2004**, *25*, 5847-5856.

15. Schuler, M.; Owen, G.R.; Hamilton, D.W.; De Wilde, M.; Textor, M.; Brunette, D.M.; Tosatti, S.G.P. Biomimetic Modification of Titanium Dental Implant Model Surfaces Using the RGDSP-Peptide Sequence: A Cell Morphology Study. *Biomaterials* **2006**, *27*, 4003-4015.
16. Fiegel, H.C.; Kaufmann, P.M.; Bruns, H.; Kluth, D.; Horch, R.E.; Vacanti, J.P.; Kneser, U. Hepatic Tissue Engineering: From Transplantation to Customized Cell-Based Liver Directed Therapies from the Laboratory. *J. Cell. Mol. Med.* **2008**, *12*, 56-66.
17. Zhu, Y.B.; Gao, C.Y.; He, T.; Shen, J.C. Endothelium Regeneration on Luminal Surface of Polyurethane Vascular Scaffold Modified with Diamine and Covalently Grafted with Gelatin. *Biomaterials* **2004**, *25*, 423-430.
18. Lee, K.K.; He, J.P.; Singh, A.; Massia, S.; Ehteshami, G.; Kim, B.; Raupp, G. Polyimide-Based Intracortical Neural Implant with Improved Structural Stiffness. *J. Micromech. Microeng.* **2004**, *14*, 32-37.
19. Richardson, R.R.; Miller, J.A.; Reichert, W.M. Polyimides as Biomaterials—Preliminary Biocompatibility Testing. *Biomaterials* **1993**, *14*, 627-635.
20. Rodriguez, F.J.; Ceballos, D.; Schuttler, M.; Valero, A.; Valderrama, E.; Stieglitz, T.; Navarro, X. Polyimide Cuff Electrodes for Peripheral Nerve Stimulation. *J. Neurosci. Method.* **2000**, *98*, 105-118.
21. Navarro, X.; Calvet, S.; Rodriguez, F.J.; Stieglitz, T.; Blau, C.; Buti, M.; Valderrama, E.; Meyer, J.U. Stimulation and Recording from Regenerated Peripheral Nerves through Polyimide Sieve Electrodes. *J. Peripher. Nerv. Syst.* **1998**, *3*, 91-101.
22. Navarro, X.; Valderrama, E.; Stieglitz, T.; Schuttler, M. Selective Fascicular Stimulation of the Rat Sciatic Nerve with Multipolar Polyimide Cuff Electrodes. *Restor. Neurolog. Neurosci.* **2001**, *18*, 9-21.
23. Dubruel, P.; Unger, R.; Van Vlierberghe, S.; Cnudde, V.; Jacobs, P.J. S.; Schacht, E.; Kirkpatrick, C.J. Porous Gelatin Hydrogels: 2. *In vitro* Cell Interaction Study. *Biomacromolecules* **2007**, *8*, 338-344.
24. Van Vlierberghe, S.; Cnudde, V.; Dubruel, P.; Masschaele, B.; Cosijns, A.; De Paepe, I.; Jacobs, P.J.S.; Van Hoorebeke, L.; Remon, J.P.; Schacht, E. Porous Gelatin Hydrogels: 1. CRYOGENIC Formation and Structure Analysis. *Biomacromolecules* **2007**, *8*, 331-337.
25. Van Vlierberghe, S.; Dubruel, P.; Lippens, E.; Cornelissen, M.; Schacht, E. Correlation between Cryogenic Parameters and Physico-Chemical Properties of Porous Gelatin Cryogels. *J. Biomater. Sci.-Polym. Ed.* **2009**, *20*, 1417-1438.
26. Van Vlierberghe, S.; Dubruel, P.; Lippens, E.; Masschaele, B.; Van Hoorebeke, L.; Cornelissen, M.; Unger, R.; Kirkpatrick, C.J.; Schacht, E. Toward Modulating the Architecture of Hydrogel Scaffolds: Curtains *versus* Channels. *J. Mater. Sci.-Mater. Med.* **2008**, *19*, 1459-1466.
27. Van Vlierberghe, S.; Sirova, M.; Rossmann, P.; Thielecke, H.; Boterberg, V.; Rihova, B.; Schacht, E.; Dubruel, P. Surface Modification of Polyimide Sheets for Regenerative Medicine Applications. *Biomacromolecules* **2010**, *11*, 2731-2739
28. Dubruel, P.; Vanderleyden, E.; Bergada, M.; De Paepe, I.; Chen, H.; Kuypers, S.; Luyten, J.; Schrooten, J.; Van Hoorebeke, L.; Schacht, E. Comparative Study of Silanisation Reactions for the Biofunctionalisation of Ti-Surfaces. *Surf. Sci.* **2006**, *600*, 2562-2571.

29. Ferris, D.M.; Moodie, G.D.; Dimond, P.M.; Gioranni, C.W.D.; Ehrlich, M.G.; Valentini, R.F. RGD-Coated Titanium Implants Stimulate Increased Bone Formation *In Vivo*. *Biomaterials* **1999**, *20*, 2323-2331.
30. MacDonald, D.E.; Rapuano, B.E.; Deo, N.; Stranick, M.; Somasundaran, P.; Boskey, A.L. Thermal and Chemical Modification of Titanium-Aluminum-Vanadium Implant Materials: Effects on Surface Properties, Glycoprotein Adsorption, and MG63 Cell Attachment. *Biomaterials* **2004**, *25*, 3135-3146.
31. Weng, Y.J.; Ren, J.R.; Huang, N.; Wang, J.; Chen, J.Y.; Leng, Y.X.; Liu, H.Q. Surface Engineering of Ti-O Films by Photochemical Immobilization of Gelatin. *Mater. Sci. Eng. C-Biomim. Supramol. Syst.* **2008**, *28*, 1495-1500.
32. Kuangl, H.G.; Kuang, Y.Y.; Chen, Z.H.; Wu, Z.H.; Jiang, B. Gelatin Immobilization on Titanium Surface by Gamma Irradiation. In *Bioceramics, Volume 20*; Daculsi, G., Layrolle, P., Eds.; Trans Tech Publications Ltd.: Stafa-Zurich, Switzerland, 2008; Parts 1 and 2, Volume 361-363, pp. 685-688.
33. Huang, C.Y.; Lu, W.; W.L.; Feng, Y.C. Effect of Plasma Treatment on the AAc Grafting Percentage of High-Density Polyethylene. *Surf. Coating. Technol.* **2003**, *167*, 1-10.
34. Van den Bulcke, A.I.; Bogdanov, B.; De Rooze, N.; Schacht, E.H.; Cornelissen, M.; Berghmans, H. Structural and Rheological Properties of Methacrylamide Modified Gelatin Hydrogels. *Biomacromolecules* **2000**, *1*, 31-38.
35. Yan, M.D.; Cai, S.X.; Wybourne, M.N.; Keana, J.F.W. Photochemical Functionalization of Polymer Surfaces and the Production of Biomolecule-Carrying Micrometer-Scale Structures by Deep-UV Lithography Using 4-Substituted Perfluorophenyl Azides. *J. Amer. Chem. Soc.* **1993**, *115*, 814-816.
36. Cai, S.X.; Kanskar, M.; Wybourne, M.N.; Keana, J.F.W. Introduction of Functional-Groups into Polymer-Films via Deep-UV Photolysis or Electron-Beam Lithography—Modification of Polystyrene and Poly(3-octylthiophene) by a Functionalized Perfluorophenyl Azide. *Chem. Mater.* **1992**, *4*, 879-884.
37. Harmer, M.A. Photomodification of Surfaces Using Heterocyclic Azides. *Langmuir* **1991**, *7*, 2010-2012.
38. Roger, P.; Renaudie, L.; Le Narvor, C.; Lepoittevin, B.; Bech, L.; Brogly, M. Surface Characterizations of Poly(ethylene terephthalate) Film Modified by a Carbohydrate-Bearing Photoreactive Azide Group. *Eur. Polym. J.* **2010**, *46*, 1594-1603.
39. Low, B.T.; Chung, T.S.; Chen, H.; Jean, Y.-C.; Pramoda, K.P. Tuning the Free Volume Cavities of Polyimide Membranes via the Construction of Pseudo-Interpenetrating Networks for Enhanced Gas Separation Performance. *Macromolecules* **2009**, *42*, 7042-7054.
40. Guerra, N.B.; Gonzalez-Garcia, C.; Llopis, V.; Rodriguez-Hernandez, J.C.; Moratal, D.; Rico, P.; Salmeron-Sanchez, M. Subtle Variations in Polymer Chemistry Modulate Substrate Stiffness and Fibronectin Activity. *Soft Matter* **2010**, *6*, 4748-4755.
41. Van Vlierberghe, S.; De Wael, K.; Buschop, H.; Adriaens, A.; Schacht, E.; Dubruel, P. Ozonation and Cyclic Voltammetry as Efficient Methods for the Regeneration of Gelatin-Coated SPR Chips. *Macromol. Biosci.* **2008**, *8*, 1090-1097.

42. Prystupa, D.A.; Donald, A.M. Infrared Study of Gelatin Conformations in the Gel and Sol States. *Polym. Gels Netw.* **1996**, *4*, 87-110.
43. Jackson, M.; Choo, L.P.; Watson, P.H.; Halliday, W.C.; Mantsch, H.H. Beware of Connective-Tissue Proteins—Assignment and Implications of Collagen Absorptions in Infrared-Spectra of Human Tissues. *Biochim. Biophys. Acta-Mol. Basis Dis.* **1995**, *1270*, 1-6.

© 2011 by the authors; licensee MDPI, Basel, Switzerland. This article is an open access article distributed under the terms and conditions of the Creative Commons Attribution license (<http://creativecommons.org/licenses/by/3.0/>).